

Research Paper

A comparative study of hopping length and allied parameters of Li⁺ ions substituted Mn²⁺/Co²⁺ ferrite nanoparticles

Ram Kadam
Research Guide
NIMS, University, Jaipur
Rajasthan

BiradarAshok Ramrao
Research Scholar,
NIMS, University, Jaipur
Rajasthan.

ABSTRACT

Li⁺ substituted CoFe₂O₄ and MnFe₂O₄ nano particles were synthesized by sol-gel auto-combustion method. The samples were obtained by annealing at relatively low temperature at 600 °C and characterized by X-ray diffraction (XRD). Lattice constant is increases with increasing Li⁺ substitution in both the systems. Hopping length is higher in Li-Mn system as compared to Li-Co ferrite system. All the allied parameters such as tetrahedral bond (d_{AX}), octahedral bond (d_{BX}), tetra edge (d_{AXE}) and octahedral edge (d_{BXE}) shows increasing trend in both the Li-Mn and Li-Co ferrite systems.

KEYWORDS: Ferrites; Sol-gel method, Hopping length.

INTRODUCTION

Manganese ferrite (MnFe₂O₄) has received a great attention in the area of magnetic storage device, microwave, and electronic device because it has high magnetic permeability and high electrical resistance. Many research groups have investigated to enhance the magnetic property of magnetic materials such as manganese ferrite. MnFe₂O₄ is a ferrimagnet (TN = 560 K) having the spinel structure with two inequivalent sublattices of tetrahedral (A) and octahedral [B] symmetries for the magnetic ions sites. Manganese ferrite is nearly normal but degree of inversion ranging from 7 to 20% have been reported [1]. Cobalt ferrite (CoFe₂O₄) shows the good magnetostrictive properties, magnetocrystalline anisotropy, high coercivity and moderate saturation magnetization among all the ferrite family [2]. The magnetoelastic properties of Co²⁺ in spinel ferrites are most commonly seen in magnetocrystalline anisotropy and relaxation effects. In general, Co²⁺ ions are stabilized in octahedral sites which give rise to a degenerate or near-degenerate orbital ground state. As a result, the strong spin-lattice interaction that arises from the unquenched orbital angular momentum has served to explain the high spin wave line widths [3]. Lithium ferrite is a low-cost substitute to the garnet based materials for microwave applications [4, 5] and is a promising candidate for cathode materials in rechargeable lithium batteries [6, 7]. This study is put light specially on the comparative variation of the hopping length of Li⁺ ions in the CoFe₂O₄ and MnFe₂O₄ nanoparticles.

2. EXPERIMENTAL PROCEDURE

Li⁺ substituted CoFe₂O₄ and MnFe₂O₄ ferrite with a chemical formula Li_{3x}MnFe_{2-x}O₄ (Li-Mn) and Li_{3x}CoFe_{2-x}O₄ (Li-Co) (where, x = 0.0, 0.1, 0.2 and 0.3) were prepared sol-gel method. The weighed amounts of these metal nitrates were completely dissolved in distilled water and the solution was stirred for half an hour. This solution was then added to citric acid in such a way that in the final sample, the molar ratio these nitrates and citric acid become 1:3. A small amount of ammonia was drop-wise added to achieve pH of the solution 7 with stirring the solution simultaneously. The detail of sol-gel synthesis method was reported in our previous reports [8-10]. Using Cu-K radiations with wavelength 1.5406 Å, X-ray diffraction investigations was analyzed at room temperature to confirm the crystallographic phase formation of nanocrystalline ferrite material.

3. RESULTS AND DISCUSSION

The XRD pattern of the typical samples (x = 0.3), showing well-defined reflections without any ambiguity, exhibits the formation of Li_{3x}MnFe_{2-x}O₄ and Li_{3x}CoFe_{2-x}O₄ (x = 0.3) is shown in Fig. 1. As the Li⁺ concentration x is higher in these samples particularly for x = 0.3, the peaks corresponding to Li are appear in the X-ray diffraction pattern showing the formation of disordered spinel structure.

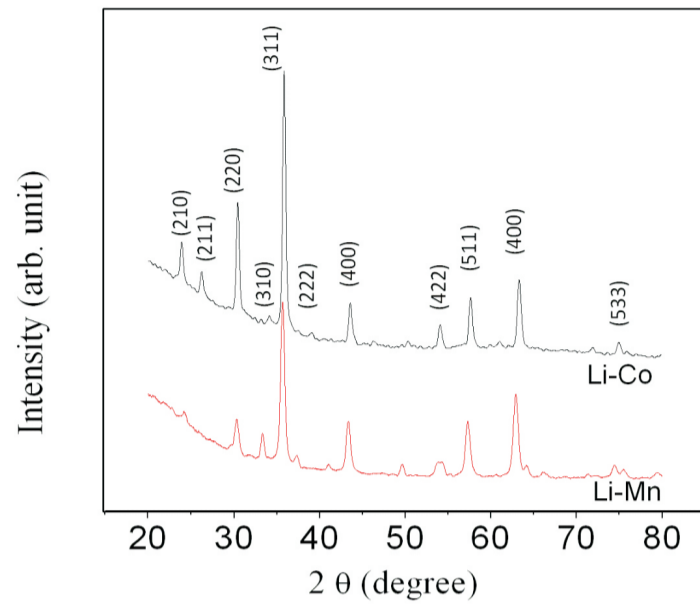


Figure 1. The XRD pattern of the typical samples (x = 0.3) of $\text{Li}_3\text{xMnFe}_2\text{-xO}_4$ and $\text{Li}_3\text{xCoFe}_2\text{-xO}_4$. The lattice parameter 'a' was calculated using the following equation [11],

$$a = d \sqrt{h^2 + k^2 + l^2} \tag{1}$$

where, d is the inter-planer spacing and (hkl) is the index of the XRD reflection peak.

The values of lattice constant was calculated for each plane and average value was taken as lattice constant for that compound and it is observed from Fig. 2 that as Li^+ concentration 'x' increases value of lattice constant increases. The radius of the Li^+ ion (0.78 \AA) is larger than that of the Fe^{3+} (0.67 \AA) thus, the lattice constant increases by the substitution of Li^+ ions for Fe^{3+} ions.

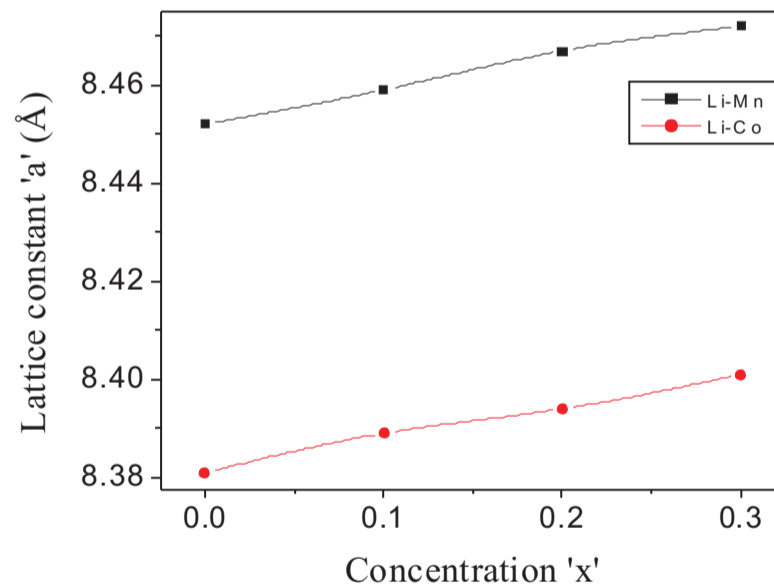


Figure 2. Variation of lattice parameter with Concentration 'x'.

Using the values of lattice constant 'a', the distance between magnetic ions (hopping lengths) available in tetrahedral A-site and octahedral B-site i.e. 'LA' and 'LB' respectively was calculated by using the relations,

$$\text{LA} = a \sqrt{3}/4 \tag{2}$$

$$\text{LB} = a \sqrt{2}/4 \tag{3}$$

Fig. 3 and 4 shows the relation between the hopping lengths in octahedral (A) and tetrahedral [B] sites as a function of Li^+ concentration x. The distance between the magnetic ions increases as the Li^+ concentration x increases. This may be attributed to the fact that the lattice constant increases with Li^+ concentration x.

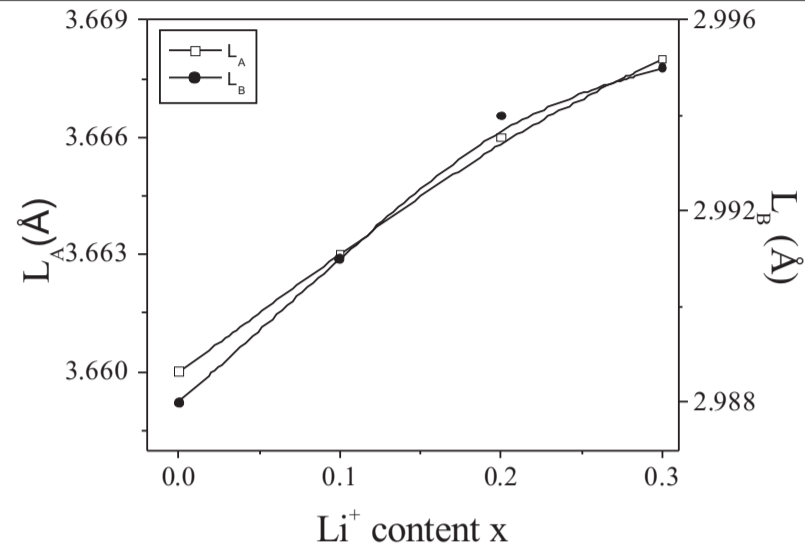


Figure 3. Variation of hopping length LA and LB for of Li₃xMnFe_{2-x}O₄

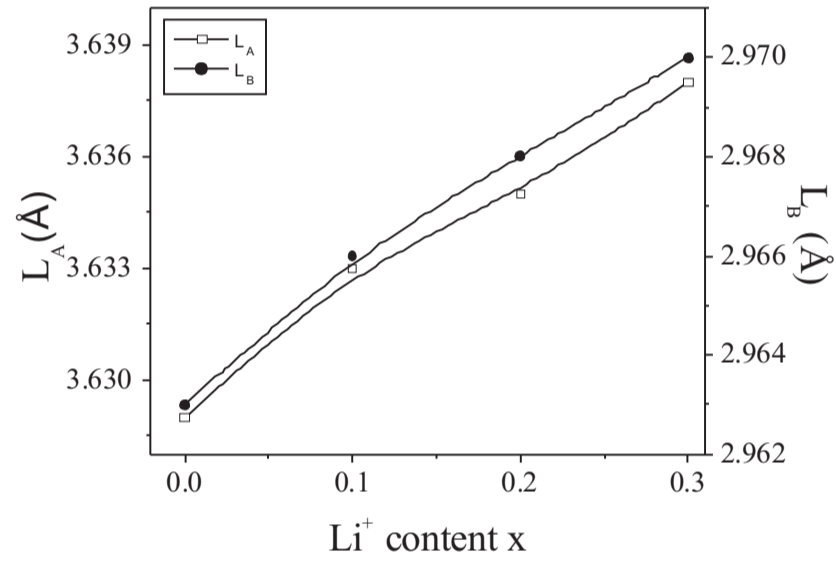


Figure 4. Variation of hopping length LA and LB for of Li₃xCoFe_{2-x}O₄

The bond length of tetrahedral A-site and octahedral B-site i.e. shortest distance between site cations and oxygen ions along with tetrahedral edge, shared and unshared octahedral edge, are calculated using the formulae given below [12] by inserting the values of lattice constant and oxygen position parameter in to these formulas.

$$d_{AX} = a\sqrt{3}u - \frac{1}{4} \quad (4)$$

$$d_{BX} = a\left(3u^2 - \frac{11}{4}u + \frac{43}{64}\right)^{\frac{1}{2}} \quad (5)$$

$$d_{AE} = a\sqrt{2} - 2u - \frac{1}{2} \quad (6)$$

$$d_{BEshared} = a\sqrt{2} - 1 - 2u \quad (7)$$

$$d_{BEunshared} = a\left(4u^2 - 3u + \frac{11}{16}\right)^{\frac{1}{2}} \quad (8)$$

The variation of these structurally important parameters are shown in the Fig. 5 and 6. It can be observed from Fig. 5 and 6 that the tetrahedral bond (d_{AX}), octahedral bond (d_{BX}), tetra edge (d_{AXE}) and octahedral edge (d_{BXE}) in both the ferrite systems are increases with increase in Li^+ substitution.

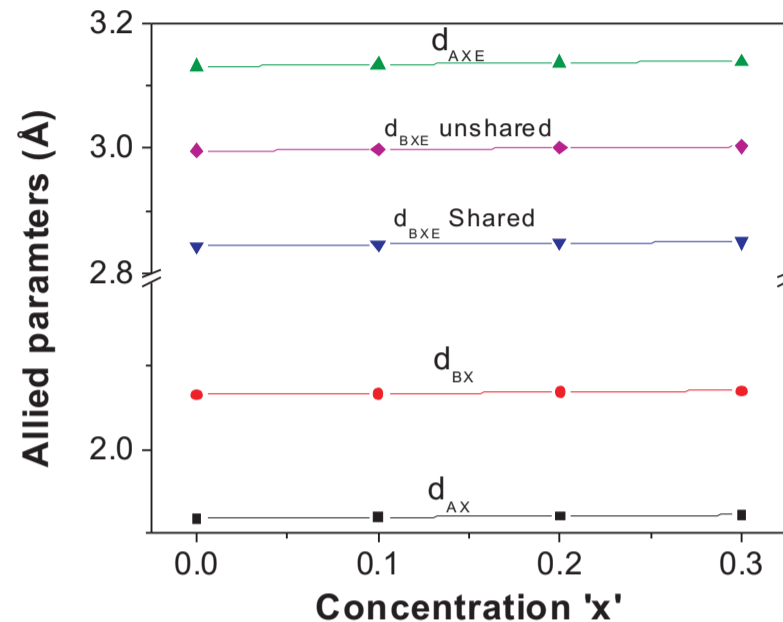


Figure 5. Allied parameters with concentration 'x' for $\text{Li}_3\text{xMnFe}_2\text{-xO}_4$

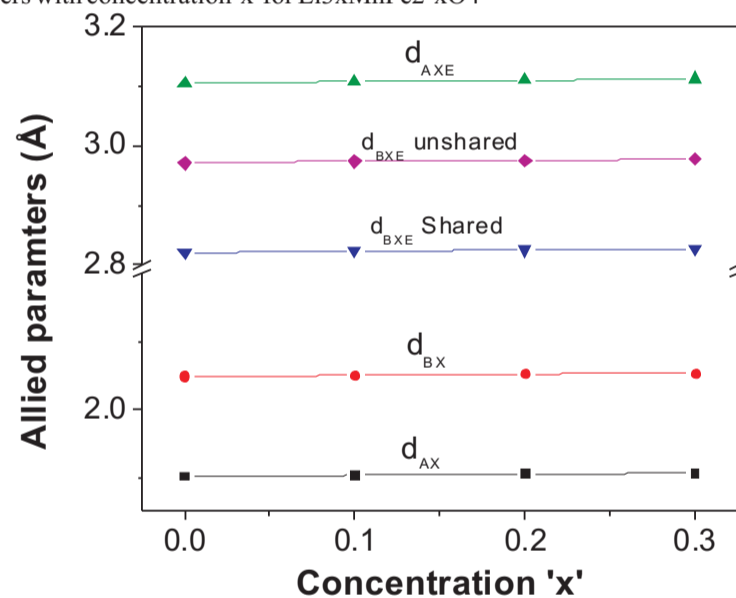


Figure 6. Allied parameters with concentration 'x' for $\text{Li}_3\text{xCoFe}_2\text{-xO}_4$

While comparing the results of both the systems it is observed that all the parameters shows increasing trend with the increasing Li^+ substitution. Further it can be noticed from the values that the Li-Mn system shows higher values as compared to Li-Co system. The higher values of all the parameter associated to Li-Mn system is mainly due to the higher lattice constant of MnFe_2O_4 .

4.CONCLUSIONS

Li^+ substituted CoFe_2O_4 and MnFe_2O_4 ferrite with a chemical formula $\text{Li}_3\text{xMnFe}_2\text{-xO}_4$ and $\text{Li}_3\text{xCoFe}_2\text{O}_4$ were successfully synthesized by sol-gel method. Li^+ ions are shows their present at higher level substitution resulting in superstructure peaks as evidence by XRD. Lattice constant is increases from 8.452 to 8.472 Å for Li-Mn system whereas in case of Li-Co system it is increases from 8.381 to 8.401Å. Li-Mn system shows higher probability of hopping between the ions as compared to Li-Co system.

REFERENCES

- [1] J.S. Hastings and L.M. Corliss, Phys. Rev. 104 (1956) 328.
- [2] B. G. Toksha, Sagar E. Shirsath, S.M. Patange, K.M. Jadhav, Solid State Commun. 147 (2008) 479-483
- [3] J.M. Song, J.G. Koh, J. Magn. Mater. 152 (1996) 383-386

- [4] **L.A. de Picciotto and M.M. Thackeray**, Mater. Res. Bull. 21 (1986) 583.
[5] **Y. Sakurai, H. Arai, and J. Yamaki**, Solid State Ionics 113-115, (1998) 29.
[6] **J. R. Dahn, U. Vom Sacken, and C.A. Michal**, Solid State Ionics 44 (1990) 87.
[7] **Sung Yong An, In-Bo Shim, and Chul Sung Kim**, J. Magn. Magn. Mater. 290 (2005) 1551.
[8] **B. G. Toksha, Sagar E. Shirsath, M. L. Mane, S. M. Patange, S. S. Jadhav, and K. M. Jadhav**, J. Phys. Chem. C, 115 (2011) 20905.
[9] **D. R. Mane, D. D. Birajdar, Swati Patil, Sagar E. Shirsath, and R. H. Kadam**, J. Sol-Gel Sci. Technol. 58 (2011) 70.
[10] **A.A. Birajdar, Sagar E. Shirsath, R.H. Kadam, S.M. Patange, K.S. Lohar, D.R. Mane, and A.R. Shitre**, J. Alloy. Compd. 512 (2012) 316.
[11] **B. D. Cullity**, Elements of X-ray diffraction, (Addison-Wesley, London, 1959)
[12] **Santosh S Jadhav, Sagar E. Shirsath, B. G. Toksha, S. M. Patange, S. J. Shukla, K. M. Jadhav**, Inter. J. Mod. Phys. B 23 (30) (2009) 5629-5638.